

Advances in Raman mapping of works of art[†]

Polonca Ropret,^{a,b} Costanza Miliani,^c Silvia A. Centeno,^{d*} Ćrtomir Tavzes^{a,b} and Francesca Rosi^e

Raman mapping can provide molecular information to complement data derived from other analytical techniques in works of art and other objects of cultural significance. Raman mapping can be performed using a motorized microscope stage that moves a sample or an object point by point in two spatial directions. The method can be used both noninvasively in works of art that fit under a microscope objective and in microsamples when, for example, obtaining information on the samples' layering structure is necessary. This paper reports on the development of a Raman mapping approach based on a set of scanning mirrors that direct the laser beam in two spatial directions, vertically through the microscope head or through a horizontal exit on the Raman microspectrometer. The first configuration still has limitations in terms of the size of the work of art that can be analyzed, as it has to fit under the microscope objective, but considerably larger objects can be studied when using the scanning mirrors placed in the horizontal exit. In this paper, the advantages and limitations of these two Raman mapping approaches are compared and discussed on the basis of an example of a contemporary oil painting on canvas. Copyright © 2010 John Wiley & Sons, Ltd.

Keywords: Raman mapping; motorized x–y stage; scanning mirrors; large works of art; noninvasive

Introduction

Raman mapping has proved to be a basic tool to gain insight into the composition of artworks' multilayered structures, such as paintings, by investigating minute stratigraphic samples (typically smaller than 1 mm³) removed from the objects. Examples of the materials and deterioration mechanisms that have been previously studied and elucidated using this mapping approach include the deterioration process of pigments in wall paintings,^[1] the painting technique of 16th century artists,^[2] rust scales on archaeological iron artifacts,^[3] the spatial distribution of corrosion products in ancient Chinese artifacts,^[4] and the composition of crusts in stained glass windows.^[5] Moreover, data from Raman mapping of microsamples have been combined with information obtained using complementary analytical techniques, including backscattered electron imaging, elemental microprobe mapping, and micro-X-ray diffraction to determine the fading mechanism of the red lead pigment in cross sections from wall paintings,^[1] elemental mapping by energy-dispersive X-ray (EDX) microanalysis to characterize pictorial layers in 16th century paintings,^[2] and backscattered electron imaging to analyze samples from corroded Chinese bronze money trees.^[4]

On the other hand, when sampling is limited or not possible at all, noninvasive Raman mapping may provide useful information on the composition and distribution of materials present at the artwork's surface. It is also possible to correlate vibrational data with information obtained from other complementary noninvasive analytical techniques, such as X-ray fluorescence (XRF) spectroscopy, open architecture X-ray diffraction (XRD), Fourier transform infrared (FTIR) reflectance spectroscopy, and ultraviolet–visible (UV–vis) reflectance spectroscopy.^[6–8] Noninvasive Raman mapping can be performed using a motorized x–y stage that moves the object in two directions in a step-by-step fashion under the microscope attached to the spectrometer. This approach has two main limitations: it can only be used with objects that fit under the microscope objective and are small enough to be moved

by the stage, and, due to the fact that the surfaces of works of art are usually not flat, is time consuming because of the automatic optimization of the focal distance that is necessary at each point.

To overcome the limitations encountered when analyzing large works of art noninvasively, a Raman mapping method based on a set of scanning mirrors that direct the laser beam in two spatial directions, vertically through the microscope head or through a horizontal exit on the Raman spectrometer, has been developed.^[9] In this approach, when the beam is directed through the microscope objective, the size of the object remains a limiting factor, but when the mirrors are placed at the spectrometer's horizontal exit, considerably larger works of art can be studied, keeping the advantages of full confocality and the possibility to use multiple excitation lines.

In the present paper, the experimental setups for both mapping approaches are presented. Examples of the application of both methods, namely noninvasive using a set of scanning mirrors and microdestructive using a motorized x–y stage, to the characterization of the artist' materials and technique in a

* Correspondence to: Silvia A. Centeno, The Metropolitan Museum of Art, New York, NY 10028, USA. E-mail: silvia.centeno@metmuseum.org

† Paper published as part of the Art and Archaeology 2009 special issue.

a Research Institute, Conservation Centre, Institute for the Protection of the Cultural Heritage of Slovenia, 1000 Ljubljana, Slovenia

b Museum Conservation Institute, Smithsonian Institution, Suitland, MD 20746, USA

c CNR-ISTM (Istituto di Scienze e Tecnologie Molecolari) c/o Dipartimento di Chimica, Università di Perugia, I-06123 Perugia, Italy

d The Metropolitan Museum of Art, New York, NY 10028, USA

e INSTM Operative Unit of Perugia c/o Dipartimento di Chimica, Università di Perugia, I-06123 Perugia, Italy

contemporary work of art are compared and discussed in the context of their capabilities and limitations.

Experimental

Raman mapping using scanning mirrors

Raman maps were obtained with a Horiba Jobin Yvon LabRAM HR800 Raman spectrometer coupled to an Olympus BXM optical microscope equipped with a scanning mirror mechanism at the horizontal exit. Measurements were made using a 785 nm laser excitation line, 10× objective lens and a 600 grooves/mm grating, which gave a spectral resolution of 0.83 cm⁻¹/pixel. The spectrometer was calibrated using the 520.5 cm⁻¹ band of a silicon wafer. The power at the samples was set to 6.6 mW using neutral density filters to avoid degradation. A multichannel air-cooled, charge-coupled device (CCD) detector was used, with integration times between 15 and 25 s. In each case, an average spectrum of the selected area was first recorded to set the optimum spectral range and integration time conditions for the subsequent step-by-step mapping. Spectra are presented after baseline correction.

Mapping modes

The experimental setup is based on a combination of mirrors that scan the laser beam along a line or over an area in the object to be studied. There are three different modes of operation: step by step, averaging and macromapping. The principle of the step-by-step mapping mode is similar to that of the traditional application using a motorized x–y stage, except that in this case the scanning mirrors move the laser beam step by step in two directions and the sample or object is kept static. At each point, a complete Raman spectrum is acquired. This mode enables high spatial resolution mapping, as the minimum scanning step is 50 nm.

In the averaging mode, the scanning mirrors oscillate allowing the generation of a macro-Raman spot (from 1 μm × 1 μm to 500 μm × 500 μm) on the selected area. As the scanning mirrors oscillate, the laser beam is raster-scanned over the objective pupil, resulting in a displacement of the laser spot on the focal plane of the objective. With a 50× objective, the laser spot is scanned at a speed of 600 μm/ms. The average shape of the laser spot becomes a square whose size can be adjusted depending on the angular amplitude of the oscillation of the scanning mirrors and the objective used. In this continuous scan mode, the energy of the laser beam is dispersed instead of concentrated in a small spot. Therefore, it is possible to carry out average Raman measurements on materials (e.g. pigments) that are prone to degrade under the laser beam, because the laser power density at the sample is lower than for the spot analysis and it depends on the size of the selected area. This mode also enables a quick acquisition of an average spectrum on the selected mapping area and can give important preliminary information on the materials present to help optimize the experimental conditions (e.g. acquisition time, spectral range) for further step-by-step, high spatial resolution mapping.

The macromapping mode is particularly useful when a quick acquisition of a Raman map is necessary over a large area. In this approach, the macro-Raman spot generated in the averaging mode is moved across the selected area of the sample step by step using the motorized x–y stage.

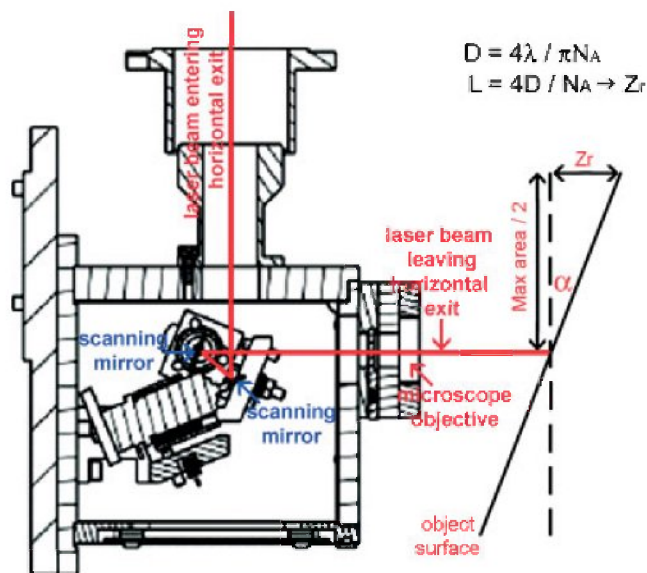


Figure 1. Sketch of the setup for Raman mapping using scanning mirrors placed at the horizontal exit, showing the incidence of the laser beam onto the artwork surface. D : lateral resolution, λ : laser beam wavelength, NA : numerical aperture of the microscope objective, L (Z_r): axial resolution, α : the angle of displacement of the artwork surface from the optimal perpendicular position, $Max\ area/2$ depends on the microscope objective aperture (e.g. $Max\ area/2 = 250\ \mu m$ when using 10× objective).

Configuration modes

The instrument can be configured to operate in two sampling modes whereby the laser beam is directed either vertically through the microscope or horizontally through the horizontal exit of the spectrometer. In the first case, scanning mirrors are placed in the microscope head and the sample can be positioned on the x–y stage or, in the case of relatively larger objects, the x–y stage can be removed and the artwork placed under the microscope objective on an additional support. This approach has limitations similar to those of the mapping approach using a motorized x–y stage in terms of the size of the work of art that can fit under the objective. In the second configuration, scanning mirrors are placed on the horizontal exit slit of the microscope, directing the laser beam to the artwork placed perpendicular to this exit (Fig. 1). Only the step-by-step and averaging modes can be used in this configuration, because in the macromapping mode the x–y stage needs to be used in combination with the averaging mode of the scanning mirror system. This approach has the advantage that the object to be studied can be larger.

In addition to its noninvasive nature, both configurations are fully confocal and do not suffer from poor coupling efficiency, in contrast to fiber-optic probes, and are compatible with multiple laser excitations, which, in the analysis of works of art, is often indispensable as the material composition is usually heterogeneous. With a fully confocal system, for example, it is possible to obtain Raman mapping data from a paint layer under a varnish layer or another organic coating.

In the setup with the scanning mirrors placed in the horizontal exit, the maximum area that can be scanned depends on the objective used, and is limited to 500 μm × 500 μm when a 10× objective is employed. This approach has limitations in terms of axial resolution, especially in cases when the surface of the artwork is not flat: for example, when a painted surface has a certain texture or when the object surface cannot be placed totally

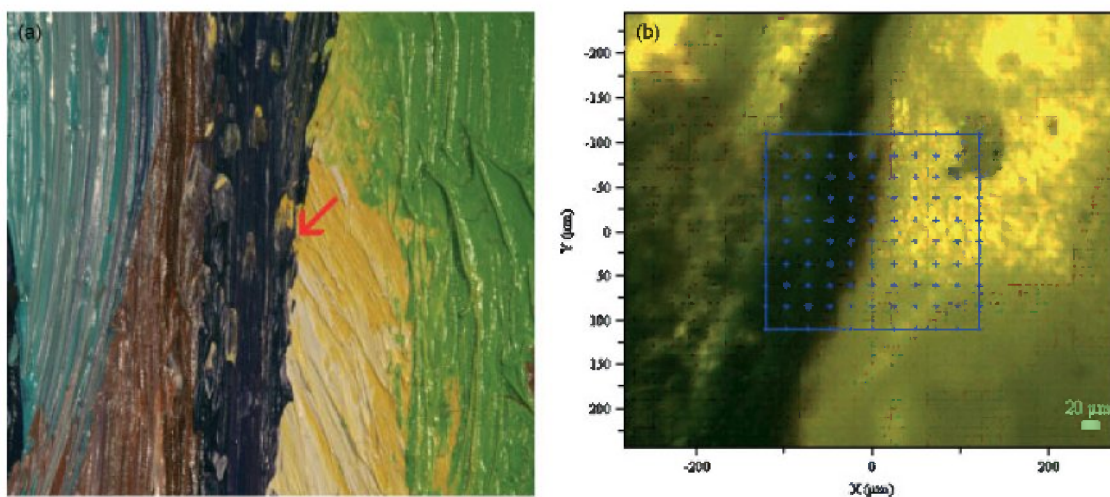


Figure 2. Photograph showing the area selected for Raman mapping on *Gola Muza/Naked Muse* in detail (a) and the same area photographed using a 10× objective lens, with a grid (240 μm × 220 μm) superimposed (b). At each point, the Raman spectrum was recorded using a 25 s integration time, 2 accumulations and a 6.6 mW power. The Raman maps acquired are presented in Fig. 4.

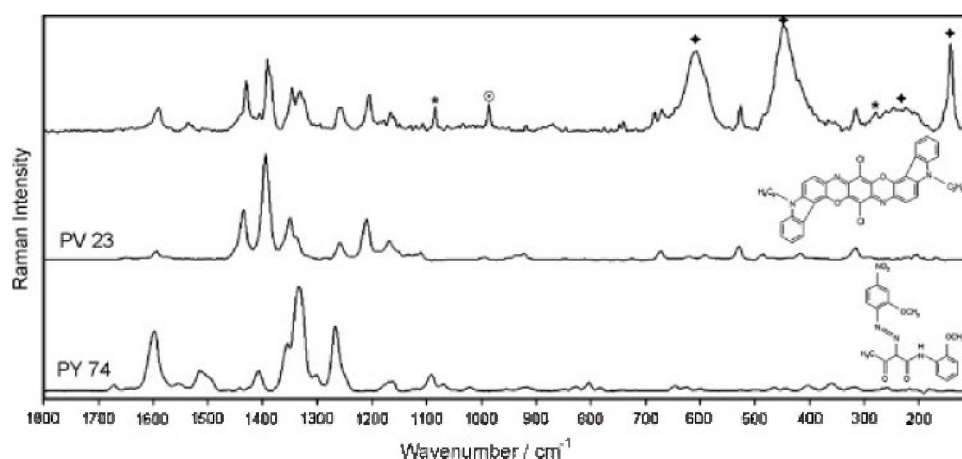


Figure 3. Average Raman spectrum recorded in the area (240 μm × 220 μm) shown in Fig. 2 (top spectrum), indicating the characteristic peaks for the inorganic pigments identified: calcite marked by *, barium white by ⊙ and titanium white (in its two forms, rutile and anatase) by ◆ Reference spectra and formulas for the synthetic organic pigments observed in the same area are also shown in this figure: PV 23 and PY 74, manufactured by Clariant and Ciba, respectively.

perpendicular to the microscope head or to the horizontal exit. The axial resolution depends on the laser excitation wavelength and on the numerical aperture of the objective used and can be easily calculated as shown in Fig. 1. For example, the maximum tolerable angle of displacement (α) of the artwork surface from the optimal perpendicular position when using a 10× objective and 785 nm laser excitation is calculated to be 6.9°.

Raman mapping using a motorized x–y stage

Micro-Raman spectra were obtained using a JASCO Ventuno double-grating spectrophotometer equipped with a CCD detector cooled to 50 °C. Raman spectra were excited using the 523 nm radiation from a Nd:YAG laser. Back illumination and collection in the backscattering geometry were made through an Olympus confocal microscope (long-focus Olympus equipped with 5×, 20×, 50× and 100× objectives). Working with a 1200 l/mm grating, it was possible to achieve a spectral resolution of about 2 cm⁻¹. The spectrometer was calibrated using the Raman lines of a polystyrene standard. In this spectrometer, the mapping capability

is provided by an automated x–y stage on which the sample is placed, and an autofocus system for z the focal position. In-plane maps were obtained with 50× and/or 100× objectives. Maps of variable dimensions were acquired by collecting spectra with a step size between 4 and 20 μm along the x and y axes. Spectral measurements were carried out with continuous scans in the 50–2000 cm⁻¹ range, exposure times between 10 and 200 s, 3–10 accumulations, and a maximum 4 mW laser power at the sample.

Results

In situ mapping using scanning mirrors

The results of *in situ* mapping measurements on the painting titled *Gola Muza/Naked Muse* (2004), 62 × 47 cm, by the artist Silvester Plotajs-Sicoe, executed on canvas in an oil technique, are discussed below. A photograph of the area, a photomicrograph, an average Raman spectrum, and the Raman maps acquired in this area are presented in Figs 2–4, showing that synthetic organic pigments (SOPs), along with inorganic extenders, were

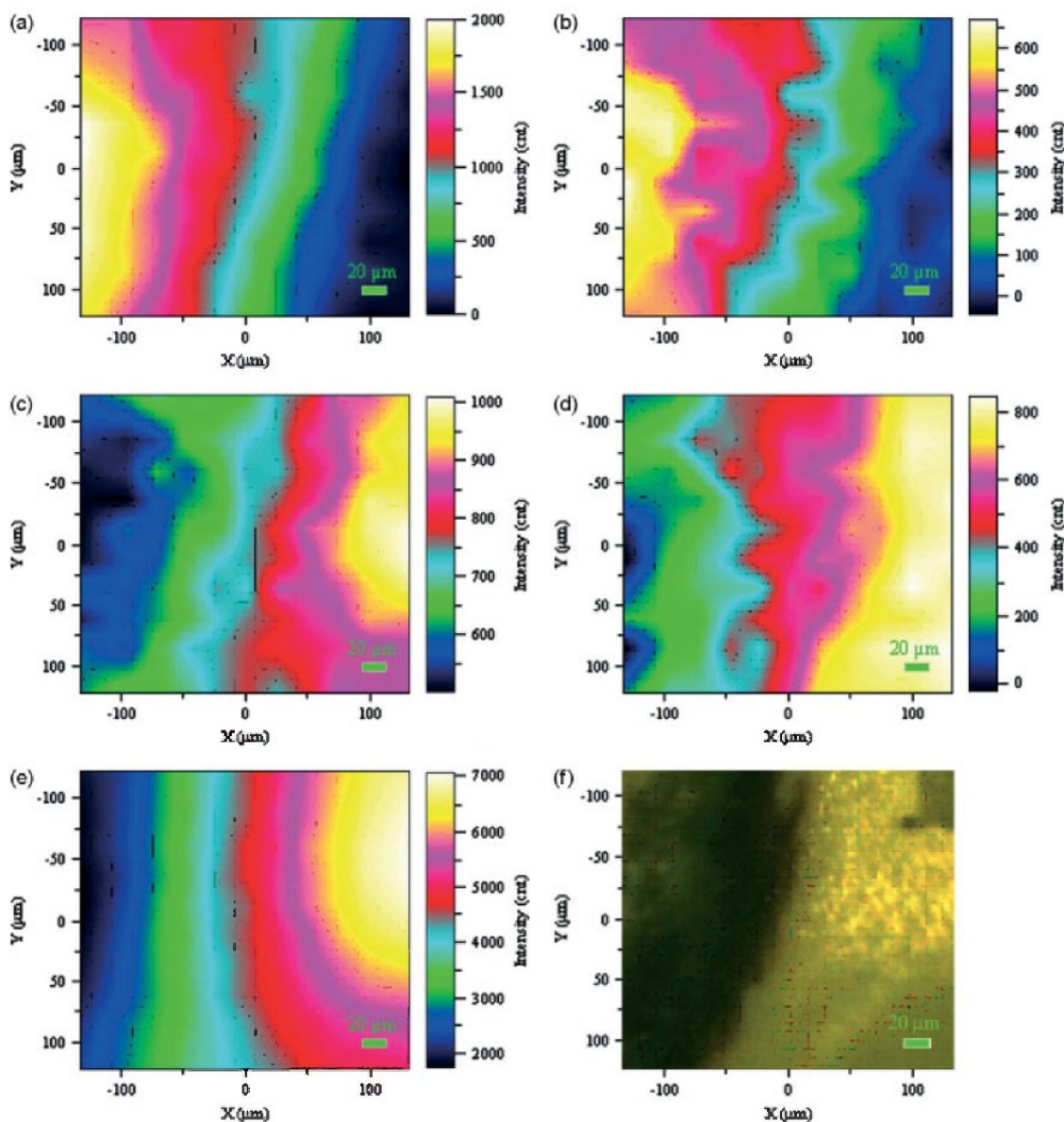


Figure 4. Individual maps for the pigments identified in the area (f), also shown in Fig. 2: PV 23 (a), barium white (b), PY 74 (c), calcite (d) and rutile (e), respectively. The distribution of rutile observed in this area perfectly matched that of anatase.

identified. The relevant modes for SOPs commonly found in works of art have been reported and discussed by several authors.^[10–13] For the step-by-step mapping mode, the 50–1800 cm^{-1} spectral range was selected, as the analysis of the bands observed below 1800 cm^{-1} is found to be sufficient to identify SOPs.^[10–14]

Figure 3 shows a Raman spectrum recorded using the averaging mode on the mapping area indicated in Fig. 2, along with reference spectra for the SOP identified: PV 23 and PY 74. Characteristic bands of PV 23, present at ca 1431, 1390, 1345, 1333, 1255, 1205, 1166, 1133, 1106, 672, and 527 cm^{-1} , are consistent with data previously published for the pigment,^[15] while bands at ca 1668, 1595, 1438, 1405, 1353, 1330, 1296, 1262, 1170, 1159, 1089, 1020, 918, 845, 825, 801 and 647 cm^{-1} are due to PY 74, in agreement with a reference spectrum previously reported.^[10] In addition to the rutile form of titanium white (TiO_2), with peaks at ca 609, 447, and 230 cm^{-1} ,^[16] the anatase form of this pigment was identified by a very strong band at ca 142 cm^{-1} , along with two other inorganic pigments,

calcite (CaCO_3) and barium white (BaSO_4), with characteristic features at ca 1086 and 987 cm^{-1} , respectively.^[16] In the spectral range below 630 cm^{-1} , it was not possible to detect the very weak bands expected for both SOPs due to the strong scattering of rutile.

Further step-by-step mapping revealed the spatial distribution of the identified pigments on the selected area (Fig. 4), indicating that the violet paint contains PV 23 and barium white, while the yellow paint is composed of PY 74 and calcite. The map distributions of the anatase (not shown) and rutile forms of TiO_2 perfectly match each other, indicating that both were present in the commercial white paint used by the artist. The distribution of titanium white does not match the violet or the yellow paints' distributions alone, suggesting that there is a layer in which TiO_2 is not mixed with any of these colored paints.

Transparent organic coatings containing, for example, waxes or natural or synthetic varnishes are very often present on the surface of works of art and archaeological objects, interfering with

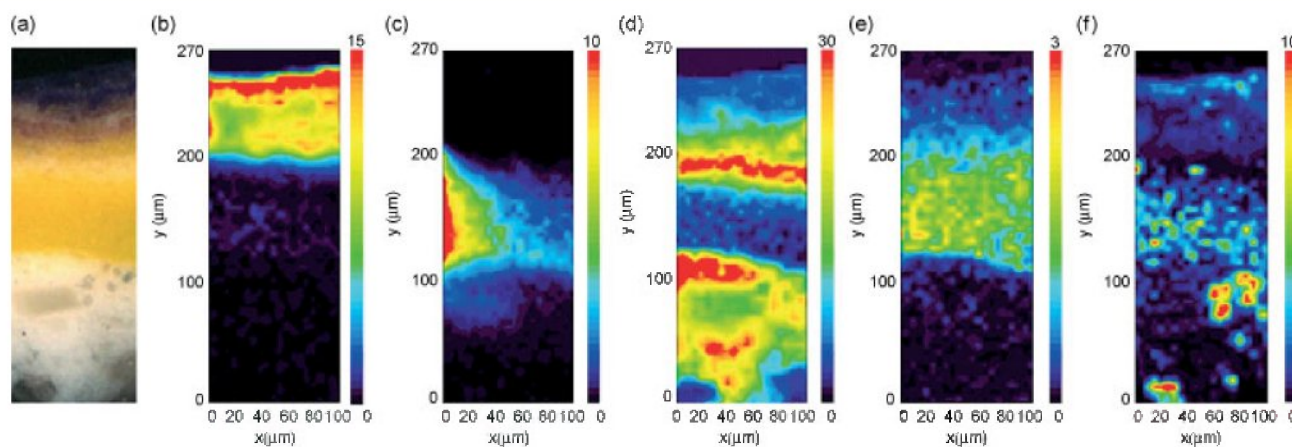


Figure 5. Photomicrograph of a sample cross section removed from the spot approximately indicated by a red arrow in *Gola Muza/Naked Muse*, in Fig. 2. Visible illumination. Original magnification 100 \times , approximate dimensions: 270 μm thick, 100 μm wide (a). Three-dimensional Raman maps (colored view) acquired in the area of the cross-section shown in (a) by mapping the characteristic bands of PV 23 at 1205 cm^{-1} (b); PY 74 at 1330 cm^{-1} (c); TiO_2 rutile at 447 cm^{-1} (d); calcite at 1086 cm^{-1} (e) and barium white at 987 cm^{-1} (f), respectively. In this sample, rutile was found to be mixed with anatase. Raman spectra were recorded using 532 nm laser excitation of 4 mW power and in 5 μm steps.

the identification of the materials below them. The ability of this mapping method to maintain full confocality offers a solution to the problem. The capability of the setup to give spectra for a paint layer under a transparent organic coating will depend on the thickness of this coating. The maximum thickness of a coating that would allow a spectrum to be recorded in an underlying paint layer can be calculated using the equations in Fig. 1, and it is, for example, ca 64 μm when using a 10 \times objective and a 785 nm excitation line.

Mapping using a motorized x – y stage

To compare both methods, a sample was removed from *Gola Muza/Naked Muse* from approximately the same area noninvasively mapped using the scanning-mirror approach (Fig. 2). A photomicrograph of a cross section of this sample is shown in Fig. 5(a). The Raman maps acquired in this sample cross section using the x – y stage are presented in the plots b–f in Fig. 5.

The results obtained are consistent with those using the scanning-mirror approach. The violet paint layer on top was found to be composed of PV 23 with relatively small amounts of barium white, by mapping, respectively, the 1205 cm^{-1} and 987 cm^{-1} characteristic bands of these compounds (Fig. 5, plots b and f), and the yellow paint layer was observed to contain a mixture of PY 74 and calcite (Fig. 5, plots c and e), by mapping the characteristic bands of PY 74 at 1330 cm^{-1} and of calcite at 1086 cm^{-1} .

This mapping approach shows that titanium white, as a uniform mixture of rutile and anatase, makes up the main pigment component in the base preparation of the painting (the map for rutile is shown in Fig. 5, plot d), and that some barium white particles are also present in this base (Fig. 5, plot f). It was also observed that barium white is mixed in the yellow paint, and that at least one paint layer containing titanium white is present in between the violet and yellow layers, though no clear boundaries are visible in the cross-section photomicrograph (plot a), suggesting that these layers were applied wet on wet. Therefore, mapping of the paint cross section using the motorized x – y stage allowed detailed information on the distribution of the different pigments in the sample stratigraphy to be obtained, which was not possible by *in situ* mapping of the surface of the artwork.

It should be stressed that the characteristic Raman bands for organic binders are almost always below the detection

limit in Raman mapping experiments. Therefore, complementary FTIR measurements could be applied for identification and characterization. Raman mapping offers unique capabilities for assessing the spatial distribution of both mineral and organic pigments within paint samples by allowing nondestructive chemical and structural mapping of heterogeneous samples with a micrometer spatial resolution. However, due to the complex composition of some paintings, it is not always possible to describe the entire stratigraphy by using a single spectroscopic method. As SEM-EDS, Raman and FTIR spectroscopies are complementary in nature, their combined use often offers the opportunity to describe heterogeneous mixtures in more detail.

Conclusions

The characterization of the compounds present on the surfaces of works of art is sometimes sufficient to address issues related to their sensitivity towards materials used in conservation–restoration treatments, such as solvents used for cleaning, to determine the most appropriate environments for exhibition and storage, or to answer questions that may arise regarding the artist's technique or the authenticity of the object. In the case of the contemporary painting discussed above, the Raman mapping approach using scanning mirrors allowed noninvasive identification of some of the pigment mixtures used by the artist that not only gave some insight into his painting technique but also provided information that is crucial to determine what solvents are appropriate for cleaning the painting's surface. Noninvasive traditional mapping is also possible using a motorized x – y stage when the art objects are small enough to fit in the microscope platform. However, to determine whether a work of art has been repainted or reworked in the past, or when information on the stratigraphy and the composition of every layer in the object is necessary to elucidate the technological process involved in its manufacture, noninvasive analyses do not give sufficient information and, therefore, sampling and detailed identification of the materials in all layers are required.

Acknowledgements

The authors would like to thank Studio Erne, Ljubljana, for lending the contemporary work of art analyzed in the present study and

especially Arnaud Zoubir, of Horiba Jobin Yvon, for the fruitful collaboration in the development of the technology behind the scanning mirror system.

References

- [1] S. Aze, J.-M. Vallet, A. Baronnet, O. Grauby, *Eur. J. Mineral.* **2006**, *18*, 835.
- [2] D. Lau, C. Willis, S. Furman, M. Livett, *Anal. Chim. Acta* **2008**, *610*, 15.
- [3] D. Neff, L. Bellot-Gurlet, P. Dillmann, S. Reguer, L. Legrand, *J. Raman Spectrosc.* **2006**, *37*, 1228.
- [4] L. I. McCann, K. Trentelman, T. Possley, B. Golding, *J. Raman Spectrosc.* **1999**, *30*, 121.
- [5] S. Murcia-Mascarós, C. Domingo, S. Sánchez-Cortés, J. V. García-Ramos, A. Muñoz-Ruiz, in *34th International Symposium on Archaeometry*, Zaragoza, Spain, **2004**, 525. <http://ifc.dpz.es/recursos/publicaciones/26/10/ebook.pdf>.
- [6] C. Miliani, F. Rosi, B. G. Brunetti, A. Sgamellotti, *Acc. Chem. Res.* **2010**, DOI: 10.1021/ar100010t.
- [7] L. B. Brostoff, S. A. Centeno, P. Ropret, P. Bythrow, F. Pottier, *Anal. Chem.* **2009**, *81*, 6096.
- [8] J. H. Townsend, L. Toniolo, F. Cappitelli (Eds), *Conservation Science 2007*, Archetype, London, **2008**, p 119.
- [9] P. Ropret, A. Zoubir, in *The Eighth Biennial Conference of the Infrared and Raman Users Group (IRUG 8)*, Vienna, Austria, **2008**, *Book of Abstracts*, p 33.
- [10] P. Vandabeele, L. Moens, H. G. M. Edwards, R. Dams, *J. Raman Spectrosc.* **2000**, *31*, 509.
- [11] P. Ropret, S. A. Centeno, P. Bukovec, *Spectrochim. Acta Part A* **2008**, *69*, 486.
- [12] F. Schulte, K.-W. Brzezinka, K. Lutzenberger, H. Stege, U. Panne, *J. Raman Spectrosc.* **2008**, *39*, 1455.
- [13] N. C. Scherrer, S. Zumbuehl, F. Delavy, A. Fritsch, R. Kuehnen, *Spectrochim. Acta Part A* **2009**, *73*, 505.
- [14] S. A. Centeno, V. Lladó Buisan, P. Ropret, *J. Raman Spectrosc.* **2006**, *37*, 1111.
- [15] J. De Gelder, P. Vandabeele, F. Govaert, L. Moens, *J. Raman Spectrosc.* **2005**, *36*, 1059.
- [16] L. Burgio, R. J. H. Clark, *Spectrochim. Acta Part A* **2001**, *57*, 1491.